Molecular Pharmacology Fast Forward. Published on July 13, 2016 as DOI: 10.1124/mol.116.104570
This article has not been copyedited and formatted. The final version may differ from this version.

Title: Synergistic Potentiation of CFTR gating by two chemically distinct potentiators, Ivacaftor (VX-770) and NPPB.

Wen-Ying Lin, Yoshiro Sohma, and Tzyh-Chang Hwang

Department of Medical Pharmacology and Physiology, Dalton Cardiovascular Research Center, University of Missouri-Columbia, Columbia, MO 65211, Department of Pharmacology, Keio University School of Medicine, Shinjuku, Tokyo 160-8582, Japan

Molecular Pharmacology Fast Forward. Published on July 13, 2016 as DOI: 10.1124/mol.116.104570
This article has not been copyedited and formatted. The final version may differ from this version.

Running title: Synergistic Potentiation of CFTR

Corresponding author:

Name: Tzyh-Chang Hwang

Mailing address: 134 Research Park Dr. Columbia, MO 65211

Telephone number: 573-882-2181

Fax number: 573-884-4232

Email address: hwangt@health.missouri.edu

The number of text pages: 42

The number of tables: 0

The number of figures: 10

The number of references: 53

The number of words in the *Abstract*: 258

The number of words in the *Introduction*: 791

The number of words in the *Discussion*: 1453

A list of nonstandard abbreviations:

VX-770 (Ivacaftor or Kalydeco): N-(2,4-ditert-butyl-5-hydroxyphenyl)-4-oxo-1H-quinoline-3-carboxamide

NPPB: 5-nitro-2-(3-phenylpropylamino) benzoate

PKA: Protein Kinase A

TMD: Transmembrane domain

NBD: Nucleotide binding domain

R domain: Regulatory domain

Molecular Pharmacology Fast Forward. Published on July 13, 2016 as DOI: 10.1124/mol.116.104570
This article has not been copyedited and formatted. The final version may differ from this version.

Abstract

Cystic Fibrosis (CF) is caused by loss-of-function mutations of the Cystic Fibrosis Transmembrane conductance Regulator (CFTR) gene encoding a phosphorylation-activated, but ATP-gated chloride channel. Previous studies suggested that VX-770 (ivacaftor), a CFTR potentiator now used in clinics, increases the open probability (P_o) of CFTR by shifting the gating conformational changes to favor the open channel configuration. Lately, the chloride channel blocker and CFTR potentiator NPPB was reported to enhance CFTR activity by a mechanism that exploits the ATP hydrolysis-driven, non-equilibrium gating mechanism unique to CFTR. Surprisingly however, NPPB increased the activity of non-hydrolytic G551D-CFTR, the third most common disease-associated mutation. Here, we further investigated the mechanism of NPPB's effects on CFTR gating by assessing its interaction with well-studied VX-770. Interestingly, once G551D-CFTR was maximally potentiated by VX-770, NPPB further increases its activity. However, quantitative analysis of this drug-drug interaction suggests that this pharmacological synergism is not due to independent actions of NPPB and VX-770 on CFTR gating; instead, our data support a dependent mechanism involving two distinct binding sites. This latter idea is further supported by the observation that the locked-open time of a hydrolysis-deficient mutant K1250A was shortened by NPPB, but prolonged by VX-770. In addition, the effectiveness of NPPB, but not of VX-770, was greatly diminished in a mutant whose second nucleotide-binding domain was completely removed. Interpreting these results under the framework of current understanding of CFTR gating not only reveals insights into the mechanism of action for different CFTR potentiators, but also brings us one step forward to a more complete schematic for CFTR gating.

Molecular Pharmacology Fast Forward. Published on July 13, 2016 as DOI: 10.1124/mol.116.104570
This article has not been copyedited and formatted. The final version may differ from this version.

Introduction

Cystic fibrosis (CF), caused by loss-of-function mutations of the CFTR (Cystic Fibrosis Transmembrane conductance Regulator) gene, is one of the most common life-shortening genetic diseases, affecting 1 in every 2500 newborns in Caucasian populations (Rowe et al., 2005; Zielenski and Tsui, 1995). The CFTR protein, functioning as a chloride channel that plays critical roles in water and salt transport in epithelium-lining tissues (Bear et al., 1992; Quinton and Reddy, 1991; Riordan et al., 1989), is classified as an ATP-binding cassette (ABC) protein because of its characteristic topological features: two cytosolic nucleotide-binding domains (NBDs) each preceded by a transmembrane domain (TMD). Unique to CFTR, however, is a regulatory (R) domain that connects two TMD/NBD complexes and contains multiple consensus serine/threonine residues for PKA-dependent phosphorylation (Ostedgaard et al., 2001).

Once the R domain is phosphorylated, opening and closing (gating) of the CFTR chloride channel are controlled, respectively, by ATP binding-induced dimerization and hydrolysis-catalyzed separation of the NBDs. (Hwang and Sheppard, 2009; Tsai et al., 2010; Tsai et al., 2009; Vergani et al., 2003; Vergani et al., 2005). A CFTR gating model (Fig. 1A) depicting energetic coupling between dimerization of CFTR's two NBDs and gate opening/closing in the TMDs was recently proposed (Jih and Hwang, 2012). In theory, mutations that disrupt any critical steps in this gating process may lead to CFTR dysfunction and hence cause CF. For example, the G551D mutation results in >100-fold reduction of the open probability (P_o) (Bompadre et al., 2007; Cai et al., 2006; Miki et al., 2010) due to a prevention of ATP-induced NBD dimerization (Lin et al., 2014), two rightmost horizontal transitions in Fig. 1A. A recent study suggests defects in the conformational changes of CFTR's TMDs (three vertical transitions

Molecular Pharmacology Fast Forward. Published on July 13, 2016 as DOI: 10.1124/mol.116.104570
This article has not been copyedited and formatted. The final version may differ from this version.

in Fig. 1A) may account for the much-reduced P_o observed in the R117H mutation associated with a mild form of CF (Yu et al., 2016).

In the past few years, high-throughput screening (Van Goor et al., 2009) identified a high-affinity CFTR potentiator, VX-770 (Ivacaftor or Kalydeco), which increases the P_o of G551D by 8 – 10 fold *in vitro*. Subsequent successful clinical trials (Accurso et al., 2010; Ramsey et al., 2011) led to FDA approval for the first CF therapy targeting mutant CFTR. However, how VX-770 potentiates a wide spectrum of gating mutants (Van Goor et al., 2014; Yu et al., 2012) remained unknown until recent papers that reveal the mechanisms for VX-770's effects on gating kinetics and energetics (Eckford et al., 2012; Jih and Hwang, 2013; Yeh et al., 2015). These latest studies support the idea that VX-770 acts at the interface between CFTR's TMDs and the lipid core of the membrane bilayer, and increases the P_o by shifting the three vertical gating transitions depicted in Fig. 1A to favor the open states. Of note, these detailed mechanistic studies provide a theoretical framework to help design second-generation drugs that can complement the action of VX-770. This strategy is important since, however encouraging, the VX-770–rectified P_o of G551D channels is still less than 10% of that of WT-CFTR (Jih and Hwang, 2013); but cf.(Van Goor et al., 2009). In addition, VX-770 diminishes the effects of VX-809 (Cholon et al., 2014; Veit et al., 2014), a compound designed to correct the trafficking defects of the most common pathogenic mutation ΔF508 (Van Goor et al., 2011). Although this negative impact of VX-770 on the action of VX-809 may not be as severe when VX-770 concentration is in the nanomolar range (Matthes et al., 2016), new CFTR potentiators with little drug-drug interactions seem warranted.

Molecular Pharmacology Fast Forward. Published on July 13, 2016 as DOI: 10.1124/mol.116.104570
This article has not been copyedited and formatted. The final version may differ from this version.

Among the plethora of CFTR potentiators (Barry et al., 2015; Rowe and Verkman, 2013) that may serve as candidates to complement or supplant VX-770, the arylaminobenzoate 5-nitro-2-(3-phenylpropylamino) benzoate or NPPB (Wei et al., 2005), which has long been known to the anion transport community as a chloride channel blocker (Wangemann et al., 1986), is particularly appealing. The action of NPPB is distinct from that of many other dual-action potentiators that increase the activity of CFTR at low concentrations but inhibit CFTR channel gating at high concentrations (Lansdell et al., 2000; Wang et al., 1998), as NPPB, when used at micromolar concentrations, potentiates CFTR channel gating as well as blocking the pore. In the current report, we show that although both NPPB and VX-770 effectively increase the P_o of wild-type and G551D CFTR to a similar extent, their effects differ markedly in other CFTR mutants tested. To investigate how NPPB and VX-770 work differently on CFTR gating, we quantify the combined effects of NPPB and VX-770, and compare them to the individual action of each compound. Our data suggest that these two reagents work not only through different binding sites, but also at different kinetic steps. The pharmacological and physiological implications of our results will be discussed.

Molecular Pharmacology Fast Forward. Published on July 13, 2016 as DOI: 10.1124/mol.116.104570
This article has not been copyedited and formatted. The final version may differ from this version.

Materials and Methods

Cell culture and transient expression system

We used Chinese hamster ovary (CHO) cells for all our patch-clamp experiments. Cells were grown at 37°C in Dulbecco's modified Eagle's medium and supplemented with 10% fetal bovine serum. We first transfected cells with pcDNA plasmids containing various CFTR constructs and pEGFP-C3 (Takara Bio Inc.) by using PolyFect (QIAGEN). The transfected CHO cells were then trypsinized, transferred to new 35-mm tissue dishes containing sterile glass chips, and incubated at 27°C before electrophysiological experiments done 2 - 3 d after transfection for microscopic current recordings or 4 – 6 d for macroscopic current recordings.

Mutagenesis

For site-directed mutagenesis, QuikChange XL kit (Agilent Technologies) was used according to the manufacturer's protocols. All of the DNA constructs were sequenced by the DNA Core (University of Missouri) to confirm mutation identity.

Electrophysiological recordings

We performed all the electrophysiological experiments at room temperature using an EPC9 amplifier (HEKA). Recording electrodes were made from borosilicate capillary glass with a two-step micropipette puller (Narishige). The tips of micropipettes were then polished using a homemade microforge before experiments. The resistance of polished pipettes was 1.5 - 3 MΩ for macroscopic current recordings and 4 - 5 MΩ for microscopic current recordings. After observing the seal resistance >40 GΩ, we excised membrane patches into an inside-out mode and applied 2 mM ATP with 25 IU PKA to activate CFTR until the current reached a steady-state.

Molecular Pharmacology Fast Forward. Published on July 13, 2016 as DOI: 10.1124/mol.116.104570
This article has not been copyedited and formatted. The final version may differ from this version.

The time course of this phosphorylation-dependent activation varies from patch to patch, but usually requires > 5 min to reach the maximal level. To minimize effects of dephosphorylation by membrane-associated phosphatases and to assess the degree of phosphorylation-independent rundown, 10 IU PKA was added in all other ATP-containing solutions applied thereafter. For the macroscopic current recording, the membrane potential was kept at −30 mV, whereas single-channel recordings were made at −50 mV. To obtain macroscopic I-V relationships, voltage ramps (−100 to +100 mV over duration of 1 s) were applied. The data were filtered with an eight-pole Bessel filter (LPF-8; Warner Instruments) with a 100-Hz cutoff frequency and digitized to a computer at a sampling rate of 500 Hz. For a better visual effect, we invert the inward current so that upward deflections represent channel openings. For recordings that demand fast solution changes, a perfusion system (SF-77B; Warner Instruments) with a dead time of ∼30 ms was used.

Chemicals and solution composition

The pipette solution contained (mM) 140 NMDG (N-Methyl-D-glucamine)-Cl (Fisher Biotec), 2 $MgCl_2$ (Fisher Biotec), 5 $CaCl_2$ (Fisher Biotec), and 10 HEPES (Fisher Biotec), pH 7.4 with NMDG for all of the patch-clamp experiments. This pipette solution was used routinely for all the experiments except those shown in Supplemental Figure 3, where pipettes were filled with NPPB-containing pipette solution. Cells were perfused with a bath solution having (mM) 145 NaCl (Fisher Biotec), 5 KCl (Fisher Biotec), 2 $MgCl_2$, 1 $CaCl_2$, 5 glucose (Fisher Biotec), 5 HEPES, and 20 sucrose (Fisher Biotec), pH 7.4 with NaOH (Fisher Biotec). After establishing an inside-out configuration, the patch was perfused with a standard perfusion solution (i.e.,

Molecular Pharmacology Fast Forward. Published on July 13, 2016 as DOI: 10.1124/mol.116.104570
This article has not been copyedited and formatted. The final version may differ from this version.

intracellular solution) containing (mM) 150 NMDG-Cl, 2 $MgCl_2$, 10 EGTA (Fisher Biotec), and 8 Tris (Fisher Biotec), pH 7.4 with NMDG.

MgATP and PKA were purchased from Sigma-Aldrich. MgATP was stored in 500 mM stock solutions at −20°C prepared to working concentration, and the pH was adjusted to 7.4 with NMDG. VX-770 (N-(2,4-Di-tert-butyl-5-hydroxyphenyl)-4-oxo-1,4-dihydroquinoline-3-carboxamide, Ivacaftor), provided by Prof. Robert Bridges (Rosalind Franklin University, North Chicago, IL), was stored as a 100 µM stock in DMSO at −70°C and diluted to 200 nM. NPPB (5-nitro-2-(3-phenylpropylamino)benzoate), purchased from Sigma-Aldrich, was stored as a 100 mM stock in DMSO at −20°C and diluted to 200 µM.

Data analysis and statistics

We used Igor Pro program (WaveMetrics) to measure the steady-state mean current amplitude. The current relaxation phase after NPPB removal was fitted with single exponential functions in G551D-, WT-, and ΔNBD2-CFTR using a built-in Levenberg–Marquardt-based algorithm. Two-tailed t-tests assuming equal variance were conducted with Excel (Microsoft) for all the comparisons showing statistical probability (p value). p was expressed as $*p < 0.05$, $**p < 0.01$, $***p < 0.001$ in figures. $*p < 0.05$ was considered statistically significant. Single-channel kinetic analysis for WT-CFTR was done with a program developed by Csanády (2000) (Figure 6). NPPB's effect on gating was isolated by first quantifying its pure blocking effect using a hydrolysis-deficient mutant, E1371S-CFTR (Moody et al., 2002; Vergani et al., 2003), whose P_o is close to unity whereas the single-channel conductance is unchanged suggesting that the pore was not affected by the mutation (Vergani et al., 2003). A similar strategy was employed in Csanády and Töröcsik (2014). Ramped I-V relationships of macroscopic E1371S-CFTR currents

Molecular Pharmacology Fast Forward. Published on July 13, 2016 as DOI: 10.1124/mol.116.104570
This article has not been copyedited and formatted. The final version may differ from this version.

in the presence or absence of 200 μM NPPB were obtained (see Fig. 1C). Fractional block of 73% was estimated for currents at -30 mV membrane potential, at which voltage all the experiments with NPPB were carried out. This value was then used to calculate the net gating effect of NPPB with the following mathematic derivation:

$I_{NPPB} = N \times P_{o\ (NPPB)} \times i_{NPPB}$, N: number of active channels in the patch, $P_{o\ (NPPB)}$: P_o in the presence of NPPB, i_{NPPB}: single-channel amplitude in the presence of NPPB.

$I_{control} = N \times P_{o\ (control)} \times i_{control}$, N: number of active channels in the patch, $P_{o\ (control)}$: P_o in the absence of NPPB, $i_{control}$: single-channel amplitude in the absence of NPPB.

Then, $I_{NPPB}/ I_{control} = P_{o\ (NPPB)}/ P_{o\ (control)} \times i_{NPPB}/ i_{control}$, assuming the number of active channels does not change over the experimental duration.

Since $i_{NPPB}/ i_{control} = 0.27$ based on 73% fractional block described above, assuming this fractional block is the same among all CFTR variants tested,

$P_{o\ (NPPB)}/ P_{o\ (control)} = I_{NPPB}/0.27/ I_{control}$.

Since our experimental protocol is always designed to include a control before and after NPPB treatment, our final control current amplitude will be the average of these two measurements:

Fold increase in P_o by NPPB = $[I_{NPPB}/0.27]/[(I_{control\ before} + I_{control\ after})/2]$,

where I_{NPPB} represents macroscopic currents in the presence of NPPB while $I_{control\ before}$ and $I_{control\ after}$ are respectively macroscopic current before the application of NPPB and that after washing out of NPPB. By averaging $I_{control\ before}$ and $I_{control\ after}$ for the control, we effectively minimized the effect of time-dependent changes of the current amplitude. Of note, the formula employed here to calculate fold increase of the P_o is based on two assumptions: First, the number of active channels in the membrane patch remains unchanged over the experimental duration; Second, the blocking effect of NPPB is the same among all CFTR variants tested. While the first assumption

Molecular Pharmacology Fast Forward. Published on July 13, 2016 as DOI: 10.1124/mol.116.104570
This article has not been copyedited and formatted. The final version may differ from this version.

is a common practice in patch-clamp experiments, the second one is presumably also safe as all the CFTR constructs used in the current study exhibit the same single-channel conductance suggesting an unperturbed pore where NPPB may reside. For experiments involving VX-770, as noted before (Jih and Hwang 2013), the "stickiness" of VX-770 makes it impossible to bracket our experiments with controls. Thus fold increase of the current was calculated based on the one control immediate before the application of VX-770.

Computer simulations

We developed an in-house computer program for simulating the drug effects on the gating of G551D-CFTR based on our proposed gating scheme (Supplemental Figure 4) using Intel Visual Fortran Compiler on the Windows 7 operation system (Cai et al., 2011). (See Supplements for details.)

Molecular Pharmacology Fast Forward. Published on July 13, 2016 as DOI: 10.1124/mol.116.104570
This article has not been copyedited and formatted. The final version may differ from this version.

Results

NPPB, best known as a chloride channel blocker (Wangemann et al., 1986), can be driven into the CFTR pore by hyperpolarizing voltages and hence disrupts the flow of chloride ions (Csanady and Torocsik, 2014; Zhang et al., 2000; Zhou et al., 2010). Thus, when NPPB was applied as a CFTR potentiator to an inside-patch that yields macroscopic currents of wild-type (WT) CFTR at a negative membrane potential, a net decrease of the current was observed since the potentiation of CFTR gating is effectively masked by pore blockade (Fig. 1B). To quantitatively assess the gating effects of NPPB, one has to first quantify its blocking effect and use this information to isolate NPPB's effects on gating. A simple way to measure pure block of the CFTR pore by NPPB is to apply the reagent to a channel with a P_o close to unity. The hydrolysis-deficient mutant, E1371S-CFTR (Vergani et al., 2003), offers just that as demonstrated recently (Csanady and Torocsik, 2014). Fig. 1C shows ramped I-V curves of macroscopic E1371S-CFTR currents in the presence or absence of 200 μM NPPB. As reported previously (Csanady and Torocsik, 2014), NPPB-induced block exhibits a strong voltage-dependence with more block at hyperpolarizing membrane potentials. From these I-V relationships, we calculated the percentages of blockade at given membrane potentials, and used these values to assess the net gating effect of NPPB as described in the *Materials and Methods*. Once the magnitude of block was corrected for data shown in Fig. 1B, we deduced that NPPB increases the P_o of WT-CFTR by 1.81 ± 0.14 fold (n = 8).

We next tested effects of NPPB on G551D-CFTR (Fig. 1D). In contrast to the result with WT channels (Fig. 1B), 200 μM NPPB increased the net G551D-CFTR currents, indicating that the gating effects outweighed the block for this mutant channel. Nonetheless, the existence of the

Molecular Pharmacology Fast Forward. Published on July 13, 2016 as DOI: 10.1124/mol.116.104570
This article has not been copyedited and formatted. The final version may differ from this version.

block of G551D-CFTR currents by NPPB was evidenced by the transient current increase upon sudden washout of NPPB (inset in Fig. 1D). The biphasic time course of current changes upon removal of NPPB was interpreted as a fast release of NPPB's blocking effect followed by a slow disappearance of its gating effects. Fitting the falling phase with a single exponential function yielded a time constant of 1.67 ± 0.28 s (n = 6). The lack of this transient increase of currents in WT-CFTR might be due to a high P_o at 2 mM ATP so that the smaller transient was masked by the low bandwidth of recording. Again, once the NPPB-induced block was corrected, we observed an increase of the P_o by 12.1 ± 1 fold (n = 20) for G551D-CFTR. These results intrigued us not only because of the differences in fold increase between WT- and G551D-CFTR, but also because NPPB could work on G551D-CFTR at all as previous studies (Csanady and Torocsik, 2014) suggest a mechanism for NPPB's action that should not be applicable for this mutant whose gating does not involve ATP hydrolysis (Lewis et al., 2004; Lin et al., 2014; Xu et al., 2014).

To further understand how NPPB modulates G551D-CFTR gating, we first reviewed briefly our previous gating scheme for G551D-CFTR (Lin et al., 2014). As the lack of a side chain at position 551 in WT-CFTR exposes the peptide backbone amide to form a hydrogen bond with the γ-phosphate of ATP upon NBD dimerization, we proposed that with a negative charge introduced at this position, NBD dimerization is likely prohibited as a result of simple electrostatic repulsion between two negatively charged entities. Of note, this idea is supported by the observation that G551E, but not G551K, exhibits a similar gating abnormality as G551D (Lin et al., 2014). We therefore modified the gating scheme (Fig. 1A) originally proposed for WT-CFTR (Jih et al., 2012a) by eliminating NBD-dimerized states to explain G551D-induced gating

Molecular Pharmacology Fast Forward. Published on July 13, 2016 as DOI: 10.1124/mol.116.104570
This article has not been copyedited and formatted. The final version may differ from this version.

defects (Fig. 2A). The resulting scheme contains two open and two closed states, "monoliganded" and "biliganded", in equilibrium. Unlike classical ligand-gated channels, however, binding of the ligand ATP by itself does not alter gating parameters of CFTR (Vergani et al., 2005). Thus, once the NBD dimerization is removed from the scheme, gating with only ATP binding/unbinding is inefficient as happened in G551D-CFTR. Nonetheless, this four-state gating scheme predicts that altering [ATP] can change the distribution of the states. As our previous study (Lin et al., 2014) suggests that 20 μM ATP can effectively decrease ATP binding to site 2 in G551D-CFTR, we examined the effects of 200 μM NPPB in the presence of 20 μM ATP (Fig. 2B). Again, NPPB increased the net current resulting in an increase of the P_o by 7.31 ± 0.81 fold (n = 3), which was significantly lower than that at 2 mM ATP ($p < 0.005$)(Fig. 2D).

To further lower the probability of occupancy in site 2, we mutated Y1219, a residue involved directly in binding of ATP at the head subdomain of NBD2 (Zhou et al., 2006), to glycine (Y1219G). We then applied 200 μM NPPB to G551D/Y1219G-CFTR in the presence of 20 μM ATP (Fig. 2C). The calculated increase of the P_o turned out to be 6.83 ± 1.53 fold (n = 8), very similar to the magnitude seen with G551D-CFTR at 20 μM ATP (Fig. 2D). If we accept the premise that our strategies have effectively eliminated the states with ATP bound in site 2, this result leads to the propositions that NPPB potentiates $C_2 \leftrightarrow O_2$ transition, and that NPPB works on this transition not as well as it affects C_2 ATP $\leftrightarrow$ O_2 ATP transition. Regardless, the above idea dictates that NPPB affects the same kinetic steps potentiated by VX-770, a well-studied CFTR potentiator (Eckford et al., 2012; Jih and Hwang, 2013; Yeh et al., 2015).

If the hypothesis that NPPB and VX-770 act on the same kinetic step is correct, we can consider

Molecular Pharmacology Fast Forward. Published on July 13, 2016 as DOI: 10.1124/mol.116.104570
This article has not been copyedited and formatted. The final version may differ from this version.

three possible scenarios: First, they bind to the same site (i.e., a competitive relationship). Second, they bind to different sites and work independently, a scenario demonstrated for nitrate and VX-770 (Yeh et al., 2015). Third, although they bind to two different sites, the effect of one drug may influence that of the other (i.e., a dependent action or drug-drug interactions). For the first scenario, when both drugs are used at saturating concentrations in our experiments, we would predict a lack of additive effects in gating potentiation upon applications of NPPB and VX-770 together. However, the experimental result contradicted this prediction (Fig. 3A & 3B). The current of G551D-CFTR was further enhanced as we added VX-770 to the bath in the presence of NPPB and vice versa. For the second scenario to be valid, one would expect that the fold increase of P_o by one reagent should be independent of the presence of the other compound. Yet, quantitative analyses of our results indicated that, at 2 mM ATP, the fold increase of NPPB did depend on the presence of VX-770 and vice versa (Fig. 3D): In the presence of NPPB, VX-770 increased the P_o of G551D-CFTR by 4.76 ± 1.75 fold (n = 5), significantly smaller than the effect of VX-770 in the absence of NPPB (9.32 ± 1.42 fold, n = 21, $p < 0.05$). Similarly, the presence of VX-770 significantly dampened the effect of NPPB (6.27 ± 1.0 fold, n = 9, vs 12.1 fold, $p < 0.005$). Thus, the overall 46-fold increase of G551D-CFTR currents when NPPB and VX-770 were applied together (46.6 ± 8.5 fold, n = 18) was larger than the sum of the effects from individual reagents (~12-fold), an indication of pharmacological synergism supporting the notion that NPPB and VX-770 bind to different sites. However, the fact that the combined effects of NPPB and VX-770 are smaller than the product of individual effects (~110-fold) suggests a mechanism by which these two potentiators work in a *dependent* manner (i.e., the third scenario described above). While the mechanism responsible for this drug-drug interaction is unclear, we can at least test one simple idea that binding of one drug lowers the effect of the other by

Molecular Pharmacology Fast Forward. Published on July 13, 2016 as DOI: 10.1124/mol.116.104570
This article has not been copyedited and formatted. The final version may differ from this version.

reducing its binding affinity. This hypothesis predicts that this "interference" can be overcome by raising the concentration of the compound of interest. Due to the limited solubility of NPPB, we were only able to increase the concentration of VX-770. As shown in Supplemental Figure 1, no further increase in G551D-CFTR currents was seen when we switched from 200 nM VX-770 to 1 μM VX-770 (1.02 ± 0.04 fold, n = 7, Supplemental Figure 1B). Thus, binding of NPPB does not appear to lower the binding affinity of VX-770.

As described above, by lowering [ATP] to 20 μM, we can shift the distribution of G551D-CFTR towards monoliganded states. Similar to the result with NPPB (Fig. 2B), the effect of VX-770 was retained but reduced (4.79 ± 1.04 fold, n = 14, Fig. 3C & D; vs. 7.31 ± 0.81 fold in Fig. 2D above). Furthermore, the inter-dependency of the effects of VX-770 and NPPB on G551D-CFTR could still be observed. In the presence of VX-770, NPPB gave only 5.0 ± 0.4 fold increase (n = 13, Fig. 3C); whereas VX-770 enhanced the P_o of NPPB-treated G551D-CFTR by 2.53 ± 0.31 fold (n = 3). When the two reagents were applied together, at 20 μM ATP, we obtained an 18.0 ± 5.0 fold increase of the P_o for G551D-CFTR (n = 7, Fig. 3C & D). Again, 18 is larger than the sum of individual effects (4.79 and 7.31 fold-increase respectively), but smaller than the product of 4.79 and 7.31, affirming pharmacological synergism between VX-770 and NPPB through a "dependent" mechanism.

This dependent mechanism between VX-770 and NPPB could also be observed in the most common pathogenic mutation ΔF508. As shown in Supplemental Figure 2A, macroscopic ΔF508-CFTR currents increase immediately upon applying NPPB with a calculated fold increase in P_o of 5.52 ± 2.18 fold (n = 10) in the presence of 2 mM ATP. However, once the activity is

Molecular Pharmacology Fast Forward. Published on July 13, 2016 as DOI: 10.1124/mol.116.104570
This article has not been copyedited and formatted. The final version may differ from this version.

enhanced by VX-770, the application of NPPB causes a net decrease of the macroscopic currents (Supplemental Figure 2B) with a calculated fold increase in P_o of 2.29 ± 0.17 fold (n = 14). While previous reports (Kopeikin et al., 2014; Van Goor et al., 2009) show a 5 – 10 fold increase of the P_o of ΔF508-CFTR by VX-770; here, in the presence of NPPB, the effect of VX-770 is decreased to 3.51 ± 1.27 fold (n = 3). In these three patches, an overall 19.4 ± 7.0 fold (n = 3) increase in P_o is seen with VX-770 and NPPB applied together (Supplemental Figure 2C).

Previous studies (Csanady and Torocsik, 2014; Jih and Hwang, 2013) demonstrated that NPPB and VX-770 share similar kinetic effects on WT-CFTR gating: an increase of the opening rate but a decrease of the closing rate, and the data presented above also show a similar magnitude of potentiation on G551D channels for both reagents. However, the fact that the effect of VX-770 and NPPB together on G551D-CFTR is larger than the sum of individual effects from each reagent when applied alone argues that VX-770 and NPPB bind to different sites in CFTR. Results in Fig. 4 further support the proposition that NPPB and VX-770 work differently. Although NPPB is considered a CFTR potentiator, Csanády and Töröcsik (2014) showed that the locked-open time of K1250A-CFTR, a hydrolysis deficient mutant, is paradoxically shortened by NPPB. In contrast, VX-770 prolongs the lock-open time of a different hydrolysis-deficient mutant E1371S-CFTR (Jih et al., 2011). To rule out the possibility of mutation-specific effect, we compared NPPB and VX-770 on K1250A-CFTR. Fig. 4A shows a representative current relaxation of K1250A-CFTR upon removal of ATP. The current decay phase could be well fitted with a single exponential function with a time constant of 54.1 s (mean data: 55.6 ± 4.3 s, n = 19). A similar experiment was carried out with the addition of VX-770 (Fig. 4B), which significantly ($p < 0.001$) prolonged the time course of current relaxation upon ATP removal (time constant =

Molecular Pharmacology Fast Forward. Published on July 13, 2016 as DOI: 10.1124/mol.116.104570
This article has not been copyedited and formatted. The final version may differ from this version.

93.2 ± 12.4 s, n = 9). On the contrary, Fig. 4C shows that NPPB indeed shortened the relaxation time constant of K1250A-CFTR to 26.9 ± 3.0 s (n = 9, $p < 0.001$). Fig. 4D summarizes current relaxation time constants for the indicated experimental conditions.

The other mutation ΔNBD2-CFTR, a construct with the NBD2 deleted and hence unresponsive to ATP (Cui et al., 2007) was also tested. As demonstrated previously, the P_o of this mutant is extremely low (Yeh et al., 2015). But, since the mutation eliminates NBD dimerization and ATP hydrolysis, the gating of ΔNBD2-CFTR can be described by an open-closed, two-state scheme in equilibrium. As seen in Fig. 4E, the application of 200 μM NPPB caused a net decrease of ΔNBD2-CFTR currents. The calculated gating effect of NPPB on ΔNBD2-CFTR was only 2.56 ± 0.15 fold (n = 5), which was not only much smaller than that of G551D ($p < 0.01$), but also far from the ~10-fold increase of the P_o of ΔNBD2-CFTR by VX-770 (Yeh et al., 2015). Upon removal of NPPB, a rapid current rise followed by a slow current decay was observed. This biphasic response to NPPB removal is reminiscent of the result seen with G551D-CFTR (Fig. 1D). However, careful inspections of these current changes provided some insights regarding the interaction of NPPB with ΔNBD2-CFTR. First, fitting the decay phase with a single exponential function yielded a time course of 39.7 ± 6.7 s (n = 9), which was much longer than that of G551D. If we assume that this decay phase reflects the dissociation of NPPB from the channel, a slower decay rate of ΔNBD2-CFTR indicates a tighter binding of NPPB to ΔNBD2-CFTR. Therefore, the reduced effect of NPPB on ΔNBD2-CFTR is not due to a lower binding affinity of the reagent with the channel. Second, because of the slow decay of the current, a stable peak current could be obtained just seconds after NPPB removal. This peak amplitude reflects the gating-enhanced current with the block eliminated. Since the ratio of this peak current and the

Molecular Pharmacology Fast Forward. Published on July 13, 2016 as DOI: 10.1124/mol.116.104570
This article has not been copyedited and formatted. The final version may differ from this version.

steady-state current in the absence of NPPB is also around 2 fold, we can conclude that the calculated potentiation effect is accurate and also exclude the possibility that the ΔNBD2 mutation may somehow alter NPPB block. Fig. 4F summarizes comparisons of the gating effects between NPPB and VX-770 on two different constructs, G551D- and ΔNBD2-CFTR. Thus, while these two CFTR potentiators bear similar effects on G551D-CFTR, deletion of NBD2 dramatically dampens the effects of NPPB but not that of VX-770, a result further reinforcing the conclusion that they work through different mechanisms.

The results presented so far suggest that NPPB and VX-770 may bind to two different sites. Our previous study (Jih and Hwang 2013) proposed that VX-770 binds to CFTR's transmembrane segments since external application of VX-770 obliterates the effect of internal VX-770. Here, we tested whether NPPB exhibits similar properties as VX-770 by loading NPPB into the pipette in experiments using inside-out membrane patches . Further application of NPPB from the intracellular side still yielded 8.89 ± 2.43 fold (n = 5) increase in G551D-CFTR macroscopic current (Supplemental Figure 3A). This result suggests that most, if not all, of NPPB's gating effects come from NPPB binding to a binding site that is readily accessible from the cytoplasmic but not the extracellular side of the membrane.

Before we proceed to the discussion section, we shall ask: Are the different magnitudes of potentiation by NPPB between WT- and G551D-CFTR (Fig. 1) due to the mutation itself? In other words, although we posit that NPPB's effects on G551D-CFTR can be well explained under the same kinetic framework used for WT channels with the only required removal of post-NBD-dimerized states in Fig. 1, it remains plausible that modification of G551D-CFTR gating

Molecular Pharmacology Fast Forward. Published on July 13, 2016 as DOI: 10.1124/mol.116.104570
This article has not been copyedited and formatted. The final version may differ from this version.

by NPPB is unique for G551D itself and not related to the behavior of WT channels. This question is relevant since many of the experiments shown in the current report were carried out with G551D-CFTR, and the results were interpreted under a unified gating scheme. As a general limitation for all mutational approaches, one can seldom absolutely rule out the possibility that the observed effects are specific to the mutation itself, but in this particular case, we can at least examine if NPPB's effects on WT-CFTR gating can be magnified by maneuvers that minimize ATP-induced NBD dimerization, and hence mimicking that of G551D-CFTR. One such experimental manipulation is to lower the probability of ATP occupancy at site 2 by decreasing [ATP] and/or mutations that reduce ATP affinity at site 2. Fig. 5 shows that indeed for WT-CFTR, as [ATP] was decreased, the potentiation effect of NPPB was increased. For example, in the presence of 100 μM ATP (Fig. 5A), 20 μM ATP (Fig. 5B), 5 μM ATP (Fig. 5C), the calculated fold increases of P_o were 2.37 ± 0.17 fold (n = 7), 3.40 ± 0.24 fold (n = 5), 5.19 ± 0.60 fold (n = 8) respectively. Moreover, in the presence of 5 μM ATP, a net increase of the current upon applying NPPB was seen, a result very similar to that of G551D. We also employed a second approach to lower the probability of occupancy in site 2, by mutating Y1219 to phenylalanine (Y1219F) and carried out the same set of experiments. In the presence of 2 mM ATP (data not shown), 100 μM ATP (Fig. 5D), 20 μM ATP (data not shown), 5 μM ATP (Fig. 5E) in Y1219F-CFTR, the fold increases of P_o were 1.71 ± 0.17 fold (n = 9), 2.95 ± 0.43 fold (n = 5), 5.41 ± 0.98 fold (n = 6), 9.10 ± 1.93 fold (n = 9) respectively (Fig. 5F). Of note, we chose not to lower [ATP] further lest a significant number of channels would lose the ATP molecule bound in site 1. Although the results did not completely replicate the same magnitude of fold increase of P_o in G551D because some of the WT channels might still go through the NBD dimerization-hydrolysis pathway, these results are qualitatively consistent with the notion that the same

Molecular Pharmacology Fast Forward. Published on July 13, 2016 as DOI: 10.1124/mol.116.104570
This article has not been copyedited and formatted. The final version may differ from this version.

mechanism for NPPB's effects on G551D-CFTR may be applicable to WT channels.

Molecular Pharmacology Fast Forward. Published on July 13, 2016 as DOI: 10.1124/mol.116.104570
This article has not been copyedited and formatted. The final version may differ from this version.

Discussion

Data presented in the current manuscript support the conclusion that NPPB and VX-770 increase the activity of G551D-CFTR through different binding sites and their mechanisms of action likely differ from each other. It should be noted that this conclusion, based simply on quantitative comparisons between combined effects of these two reagents and their individual effects, is independent of any kinetic model for CFTR gating. Further evidence supporting this conclusion includes: First, relative to the magnitudes of gating potentiation by NPPB and VX-770 on G551D-CFTR, deletion of NBD2 drastically reduces the efficacy of NPPB but not that of VX-770 (Fig. 4F); Second, NPPB and VX-770 pose opposite effects on the closing rate of K1250A-CFTR (Fig. 4D); Third, while the binding site for VX-770 is equally accessible from either side of the membrane (Jih and Hwang, 2013), the one for NPPB is preferentially accessible from the cytoplasmic side of the channel. To elucidate the potential mechanism responsible for this interesting drug-drug interaction between two CFTR potentiators, it is helpful to understand our results in the context of a gating model.

The modified gating model depicted in Fig. 2A for G551D-CFTR was used to see whether we can gain some insights into the mechanism of action for NPPB, which may then shed light on how NPPB acts on WT-CFTR. As proposed originally by Vergani et al. (2003), ATP binding to the catalysis-competent site (or site 2) is not coupled to gate opening; opening of CFTR's gate is controlled instead by NBD dimerization, which is facilitated by ligand binding. Applying this concept to our gating model, we reckon that the two transitions in Fig. 2A, C_2 ATP $\leftrightarrow$ O_2 ATP and $C_2 \leftrightarrow O_2$, should share the same parameters. This lack of energetic coupling between ATP binding and gating predicts that NPPB should exert a similar effect on these two kinetic reactions

Molecular Pharmacology Fast Forward. Published on July 13, 2016 as DOI: 10.1124/mol.116.104570
This article has not been copyedited and formatted. The final version may differ from this version.

and hence the potentiation effect of NPPB should not depend on [ATP], changes of which shift the distribution of the channel between mono-liganded and bi-liganded states. Our experimental data (Fig. 2B, C, &D) apparently contradict this prediction. In order to keep the scheme unchanged, one has to propose that NPPB works differently on these two transitions: C_2 ATP $\leftrightarrow$ O_2 ATP and $C_2 \leftrightarrow O_2$.

Suppose, indeed, NPPB affects the $C_2 \leftrightarrow O_2$ step, the same transition proposed to be modulated by VX-770, we expect either a competitive relationship (i.e., binding to the same site) or an independent action from two distinct binding sites (e.g., nitrate and VX-770 in Yeh et al. (2015)) when NPPB is applied together with VX-770. However, neither was observed. Instead, a "reduction" of one reagent's effect was seen in the presence of the other reagent as if they work in a *dependent* manner. Our results also make it unlikely that this apparent negative impact of one drug over the other is due to a change of binding affinity (Supplemental Figure 1). Thus, although we cannot rule out some sort of non-specific "allosteric" interference between NPPB and VX-770, here we attempt to find a more testable proposition based on a relatively new idea of the gating mechanism of CFTR.

As shown in Fig. 1A, the energetic coupling model depicts a probabilistic relationship between NBD dimerization and gate opening. ATP, the ligand for CFTR gating, serves as a catalyst that facilitates NBD dimerization. The sheer existence of this molecular motion predicts NBD dimerization with an unoccupied site 2 (i.e., C_2 and O_2 states). We thus propose to add C_{0AD} and O_0 states representing a closed state and an open state respectively with dimerized NBDs but an empty site 2 (Fig. 6). In the absence of the catalyst ATP in site 2, transitions from C_2 and O_2 to

Molecular Pharmacology Fast Forward. Published on July 13, 2016 as DOI: 10.1124/mol.116.104570
This article has not been copyedited and formatted. The final version may differ from this version.

these two newly added states are slow, but the same principle of energetic coupling between NBD dimerization and gate opening should apply. That is, $C_{0AD} \leftrightarrow O_0$ should assume a higher P_o than $C_2 \leftrightarrow O_2$. This modification of CFTR gating scheme, albeit speculative, not only explains data presented in our previous report (Lin et al., 2014), but also opens a new possibility to explain how VX-770 and NPPB can interact with each other.

We hypothesize that NPPB, by binding at the NBD dimer interface, promotes NBD dimerization, a mechanism distinct from that of VX-770. Qualitatively, this mechanism explains how NPPB increases the opening rate of WT-CFTR (increasing $C_{2ATP} \rightarrow C_{2AD}$ in Fig. 1A), shortens the lock-open time of K1250A-CFTR presumably due to destabilization of NBD dimer because of molecular crowding, and inhibits ATP hydrolysis (Csanady and Torocsik, 2014). This hypothesis also offers a straightforward explanation for the sensitivity of NPPB's effects to the deletion of NBD2. Furthermore, this proposed mechanism also qualitatively explains an intriguing, fortuitous observation noted in Fig. 3A: the presence of NPPB reduced the initial current rising phase upon ATP washout with G551D-CFTR (46 ± 5%, n = 4, versus 70% in the presence of VX-770). As reported previously (Lin et al., 2014), this rapid current increase phase is due to G551D-CFTR channels being trapped by millimolar ATP in the C_{2ATP} states depicted in Fig. 6; whereas removal of ATP allows the CFTR protein to undergo conformational changes to the more stable dimerized open states, O_0 in the modified gating scheme. Thus, NPPB, through the proposed mechanism, shifts the gating equilibrium of G551D-CFTR channels to dimerized-O_0 and C_{0AD} states, and hence diminishes the apparent "inhibitory" action of ATP. Lastly, because of the coupling between NBD dimerization and gate opening, a dependent interaction is expected for NPPB acting on NBD dimerization and VX-770, which modulates directly gate

Molecular Pharmacology Fast Forward. Published on July 13, 2016 as DOI: 10.1124/mol.116.104570
This article has not been copyedited and formatted. The final version may differ from this version.

opening/closing step. In Supplemental Figure 4, we provide results based on computer simulations to collaborate this idea of a dependent mechanism for these two CFTR potentiators.

While results from our computer simulations are consistent with the idea that NPPB acts on NBD dimerization steps for G551D-CFTR (Supplemental Figure 4), the question is whether the same mechanism can be applied to WT-CFTR. This question is hard to answer, as one can never completely exclude the possibility of a global effect caused by the mutation on the protein structure and hence gating function. Nevertheless, as we showed in Fig 5, the potentiation effect of NPPB at very low [ATP] in WT-CFTR, which eliminates most ATP-induced NBD dimerization events to mimic G551D-CFTR, is similar to that of G551D.

Although our computer simulations using the modified gating model seem to fit some experimental data (see Fig.S3), we were unable to explain a reduction of the effect of VX-770 on G551D-CFTR when [ATP] is decreased to 20 μM (10 fold based on simulations, but 5 fold observed). Here we speculate several possible reasons responsible for this discrepancy. First, we must accept the possibility that our model is wrong. While our model does explain many of the current as well as published data, yet these inconsistent results do provide an opportunity to reexamine the model in the future.. Second, since P_o of G551D-CFTR is extremely low, most of our recordings yield microscopic currents, resulting in imprecise measurements. However, we did not see the expected large variation of our data predicted by this scenario. Third, it is a generally held principle that modeling should be carried out with as few assumptions as possible. Here, the simplest assumption for our simulations is that VX-770 affects each vertical transition to the same extent. However, it was recently shown that conformational changes in the NBDs

Molecular Pharmacology Fast Forward. Published on July 13, 2016 as DOI: 10.1124/mol.116.104570
This article has not been copyedited and formatted. The final version may differ from this version.

will cause reorientation of transmembrane domains (Ehrhardt et al., 2016), which may in theory alter the effect of VX-770 as VX-770 is proposed to bind to the transmembrane domains. Therefore, although modifications of our assumption may better suit the experimental data, we decided not to increase complexity lacking supporting evidence.

One caveat of our study we recognize is that our functional assay does not allow direct visualization of NPPB's binding site; therefore, much of what have been deliberated above remains speculative. It may also be interesting to consider the possible binding sites identified by previous studies. Moran et al. (2005) argue that the NBD1:NBD2 interface is one binding site for CFTR potentiators. Kalid et al.(2010) raise the possibility that the interface between the NBDs and the intracellular loops is another potential binding site. Indeed much more about how potentiators work on CFTR channels awaits future studies using diverse tools. Nonetheless, the current work by demonstrating synergistic effects of two well-studied CFTR potentiators and a logical gating scheme supported by numerous functional data do lay a sound foundation to guide future drug design. The unique dependent gating mechanism revealed here underscores the possibility of developing drugs that can complement the action of VX-770, and hence holds the promise of a major therapeutical advancement for at least a subset of CF patients.

Molecular Pharmacology Fast Forward. Published on July 13, 2016 as DOI: 10.1124/mol.116.104570
This article has not been copyedited and formatted. The final version may differ from this version.

Acknowledgments

We thank Cindy Chu and Shenghui Hu for their technical assistance and Dr. Robert Bridges for providing VX-770. We also thank Kang-Yang Jih for their efforts in carrying out some pilot experiments.

Molecular Pharmacology Fast Forward. Published on July 13, 2016 as DOI: 10.1124/mol.116.104570
This article has not been copyedited and formatted. The final version may differ from this version.

Authorship Contributions

Participated in research design: Lin, Sohma, Hwang.

Conducted experiments: Lin.

Contributed new reagents or analytic tools: Sohma

Performed data analysis: Lin.

Wrote or contributed to the writing of the manuscript: Lin, Sohma, Hwang.

Molecular Pharmacology Fast Forward. Published on July 13, 2016 as DOI: 10.1124/mol.116.104570
This article has not been copyedited and formatted. The final version may differ from this version.

References

Accurso FJ, Donaldson SH, Moss RB, Pilewski JM, Rubenstein RC, Uluer AZ, Aitken ML, Freedman SD, Rose LM, Mayer-Hamblett N, Dong Q, Rowe SM, Zha J, Stone AJ, Olson ER, Ordoñez CL, Campbell PW, Ashlock MA, Ramsey BW, Clancy JP, Boyle MP, Dunitz JM, Durie PR, Sagel SD, Hornick DB and Konstan MW (2010) Effect of VX-770 in Persons with Cystic Fibrosis and the G551D-CFTR Mutation. *N Engl J Med* **363**(21): 1991-2003.

Barry PJ, Ronan N and Plant BJ (2015) Cystic fibrosis transmembrane conductance regulator modulators: the end of the beginning. *Semin Respir Crit Care Med* **36**(2): 287.

Bear CE, Li C, Kartner N, Bridges RJ, Jensen TJ, Ramjeesingh M and Riordan JR (1992) Purification and functional reconstitution of the cystic fibrosis transmembrane conductance regulator (CFTR). *Cell* **68**(4): 809-818.

Bompadre SG, Sohma Y, Li M and Hwang T-C (2007) G551D and G1349D, two CF-associated mutations in the signature sequences of CFTR, exhibit distinct gating defects. *J Gen Physiol* **129**(4): 285-298.

Cai Z, Sohma Y, Bompadre SG, Sheppard DN and Hwang T-C (2011) Application of high-resolution single-channel recording to functional studies of cystic fibrosis mutants. *Methods Mol Biol* **741**: 419-441.

Cai Z, Taddei A and Sheppard DN (2006) Differential sensitivity of the Cystic Fibrosis (CF)-associated mutants G551D and G1349D to potentiators of the cystic fibrosis transmembrane conductance regulator (CFTR) Cl- channel. *J Biol Chem* **281**(4): 1970-1977.

Cholon DM, Quinney NL, Fulcher ML, Esther JCR, Das J, Dokholyan NV, Randell SH, Boucher

RC and Gentzsch M (2014) Potentiator ivacaftor abrogates pharmacological correction of ΔF508 CFTR in cystic fibrosis. *Sci Transl Med* **6**(246): 246ra296-246ra296.

Csanady L and Torocsik B (2014) Catalyst-like modulation of transition states for CFTR channel opening and closing: New stimulation strategy exploits nonequilibrium gating. *J Gen Physiol* **143**(2): 269-287.

Cui L, Riordan JR, Aleksandrov L, Chang X-B, Hou Y-X, He L, Hegedus T, Gentzsch M, Aleksandrov A and Balch WE (2007) Domain Interdependence in the Biosynthetic Assembly of CFTR. *J Mol Biol* **365**(4): 981-994.

Eckford PDW, Li CH, Ramjeesingh M and Bear CE (2012) Cystic Fibrosis Transmembrane Conductance Regulator (CFTR) Potentiator VX-770 (Ivacaftor) Opens the Defective Channel Gate of Mutant CFTR in a Phosphorylation-dependent but ATP-independent Manner. *J Biol Chem* **287**(44): 36639-36649.

Ehrhardt A, Chung WJ, Pyle LC, Wang W, Nowotarski K, Mulvihill CM, Ramjeesingh M, Hong J, Velu SE, Lewis HA, Atwell S, Aller S, Bear CE, Lukacs GL, Kirk KL and Sorscher EJ (2016) Channel Gating Regulation by the Cystic Fibrosis Transmembrane Conductance Regulator (CFTR) First Cytosolic Loop. *J Biol Chem* **291**(4): 1854-1865.

Hwang T-C and Sheppard DN (2009) Gating of the CFTR Cl- channel by ATP-driven nucleotide-binding domain dimerisation. *J Physiol* **587**(Pt 10): 2151-2161.

Jih K-Y and Hwang T-C (2012) Nonequilibrium Gating of CFTR on an Equilibrium Theme. *Physiol(Bethesda)* **27**(6): 351-361.

Jih K-Y and Hwang T-C (2013) Vx-770 potentiates CFTR function by promoting decoupling between the gating cycle and ATP hydrolysis cycle. *Proc Natl Acad Sci USA* **110**(11): 4404-4409.

Jih K-Y, Li M, Hwang T-C and Bompadre SG (2011) The most common cystic fibrosis-associated mutation destabilizes the dimeric state of the nucleotide-binding domains of CFTR. *J Physiol* **589**(Pt 11): 2719-2731.

Jih K-Y, Sohma Y and Hwang T-C (2012a) Nonintegral stoichiometry in CFTR gating revealed by a pore-lining mutation. *J Gen Physiol* **140**(4): 347-359.

Jih K-Y, Sohma Y, Li M and Hwang T-C (2012b) Identification of a novel post-hydrolytic state in CFTR gating. *J Gen Physiol* **139**(5): 359-370.

Kalid O, Mense M, Fischman S, Shitrit A, Bihler H, Ben-Zeev E, Schutz N, Pedemonte N, Thomas PJ, Bridges RJ, Wetmore DR, Marantz Y and Senderowitz H (2010) Small molecule correctors of F508del-CFTR discovered by structure-based virtual screening. *J Comput Aided Mol Des* **24**(12): 971-991.

Kopeikin Z, Sohma Y, Li M and Hwang T-C (2010) On the mechanism of CFTR inhibition by a thiazolidinone derivative. *J Gen Physiol* **136**(6): 659-671.

Kopeikin Z, Yuksek Z, Yang HY and Bompadre SG (2014) Combined effects of VX-770 and VX-809 on several functional abnormalities of F508del-CFTR channels. *J Cyst Fibros* **13**(5): 508-514.

Lansdell KA, Cai Z, Kidd JF and Sheppard DN (2000) Two mechanisms of genistein inhibition of cystic fibrosis transmembrane conductance regulator Cl− channels expressed in murine cell line. *J Physiol* **524**(2): 317-330.

Lewis HA, Hendrickson WA, Hunt JF, Kearins MC, Lorimer D, Maloney PC, Post KW, Rajashankar KR, Rutter ME, Sauder JM, Shriver S, Buchanan SG, Thibodeau PH, Thomas PJ, Zhang M, Zhao X, Emtage S, Burley SK, Conners K, Dickey M, Dorwart M, Fowler R, Gao X and Guggino WB (2004) Structure of nucleotide-binding domain 1 of

the cystic fibrosis transmembrane conductance regulator. *EMBO J* **23**(2): 282-293.

Lin W-Y, Jih K-Y and Hwang T-C (2014) A single amino acid substitution in CFTR converts ATP to an inhibitory ligand. *J Gen Physiol* **144**(4): 311-320.

Ma T, Thiagarajah JR, Yang H, Sonawane ND, Folli C, Galietta LJV and Verkman AS (2002) Thiazolidinone CFTR inhibitor identified by high-throughput screening blocks cholera toxin-induced intestinal fluid secretion. *J Clin Invest* **110**(11): 1651-1658.

Matthes E, Goepp J, Carlile GW, Luo Y, Dejgaard K, Billet A, Robert R, Thomas DY and Hanrahan JW (2016) Low free drug concentration prevents inhibition of F508del CFTR functional expression by the potentiator VX-770 (ivacaftor). *Brit J Pharmacol* **173**(3): 459-470.

Miki H, Zhou Z, Li M, Hwang T-C and Bompadre SG (2010) Potentiation of disease-associated cystic fibrosis transmembrane conductance regulator mutants by hydrolyzable ATP analogs. *J Biol Chem* **285**(26): 19967-19975.

Moody JE, Millen L, Binns D, Hunt JF and Thomas PJ (2002) Cooperative, ATP-dependent association of the nucleotide binding cassettes during the catalytic cycle of ATP-binding cassette transporters. *J Biol Chem* **277**(24): 21111-21114.

Moran O, Galietta LJV and Zegarra-Moran O (2005) Binding site of activators of the cystic fibrosis transmembrane conductance regulator in the nucleotide binding domains. *Cell Mol Life Sci* **62**(4): 446-460.

Ostedgaard LS, Baldursson O and Welsh MJ (2001) Regulation of the cystic fibrosis transmembrane conductance regulator Cl- channel by its R domain. *J Biol Chem* **276**(11): 7689-7692.

Quinton PM and Reddy MM (1991) Regulation of absorption in the human sweat duct. *Adv Exp*

Med Biol **290**: 159.

Ramsey BW, Konstan MW, Moss R, Ratjen F, Sermet-Gaudelus I, Rowe SM, Dong Q, Rodriguez S, Yen K, Ordoñez C, Elborn JS, Davies J, McElvaney NG, Tullis E, Bell SC, Dřevínek P, Griese M, McKone EF, Wainwright CE and Group VXS (2011) A CFTR potentiator in patients with cystic fibrosis and the G551D mutation. *N Engl J Med* **365**(18): 1663-1672.

Riordan JR, Rommens JM, Kerem B, Alon N, Rozmahel R, Grzelczak Z, Zielenski J, Lok S and Plavsic N, Chou J-L, Drumm ML, Iannuzzi MC, Collins FS and Tsui L-C (1989) Identification of the cystic fibrosis gene: cloning and characterization of complementary DNA. *Science* **245**(4922): 1066-1073.

Rowe SM and Verkman AS (2013) Cystic fibrosis transmembrane regulator correctors and potentiators, in *Cystic Fibrosis: A Trilogy of Biochemistry, Physiology, and Therapy* (Riordan JR, Boucher RC, and Quinton PM eds) pp 287-301, Cold Spring Harbor Publishers, New York.

Rowe SM, Miller S and Sorscher EJ (2005) MECHANISMS OF DISEASE: Cystic Fibrosis. *N Engl J Med* **352**(19): 1992.

Tsai M-F, Li M and Hwang T-C (2010) Stable ATP binding mediated by a partial NBD dimer of the CFTR chloride channel. *J Gen Physiol* **135**(5): 399-414.

Tsai M-F, Shimizu H, Sohma Y, Li M and Hwang T-C (2009) State-dependent modulation of CFTR gating by pyrophosphate. *J Gen Physiol* **133**(4): 405-419.

Van Goor F, Hadida S, Grootenhuis PD, Burton B, Cao D, Neuberger T, Turnbull A, Singh A, Joubran J, Hazlewood A, Zhou J, McCartney J, Arumugam V,Decker C, Yang J, Young C, Olson ER, Wine JJ, Frizzell RA, Ashlock M, Negulescu P. (2009) Rescue of

CF airway epithelial cell function in vitro by a CFTR potentiator, VX-770. *Proc Natl Acad Sci USA* **106**(44): 18825-18830.

Van Goor F, Olson ER, Wine JJ, Frizzell RA, Ashlock M, Negulescu PA, Hadida S, Grootenhuis PDJ, Burton B, Stack JH, Straley KS, Decker CJ, Miller M and McCartney J (2011) Correction of the F508del-CFTR protein processing defect in vitro by the investigational drug VX-809. *Proc Natl Acad Sci USA* **108**(46): 18843-18848.

Van Goor F, Yu HH, Burton B and Hoffman BJ (2014) Effect of ivacaftor on CFTR forms with missense mutations associated with defects in protein processing or function. *J Cyst Fibros* **13**(1): 29-36.

Veit G, Finkbeiner WE, Hegedus T, Verkman AS, Lukacs GL, Avramescu RG, Perdomo D, Phuan P-W, Bagdany M, Apaja PM, Borot F, Szollosi D and Wu Y-S (2014) Some gating potentiators, including VX-770, diminish ΔF508-CFTR functional expression. *Sci Transl Med* **6**(246): 246ra297.

Vergani P, Lockless SW, Nairn AC and Gadsby DC (2005) CFTR channel opening by ATP-driven tight dimerization of its nucleotide-binding domains. *Nature* **433**(7028): 876-880.

Vergani P, Nairn AC and Gadsby DC (2003) On the mechanism of MgATP-dependent gating of CFTR Cl- channels. *J Gen Physiol* **121**(1): 17-36.

Wang F, Zeltwanger S, Yang ICH, Nairn AC and Hwang T-C (1998) Actions of genistein on cystic fibrosis transmembrane conductance regulator channel gating: Evidence for two binding sites with opposite effects. *J Gen Physiol* **111**(3): 477-490.

Wang W, Li G, Clancy JP, Kirk KL (2005) Activating Cystic Fibrosis Transmembrane Conductance Regulator Channels with Pore Blocker Analogs. *J Biol Chem* **280**(25): 23622-23630.

Wangemann P, Wittner M, Di Stefano A, Englert HC, Lang HJ, Schlatter E and Greger R (1986) Cl--channel blockers in the thick ascending limb of the loop of Henle Structure activity relationship. *Pflug Arch Eur J Phy* **407**(2): S128-S141.

Xu Z, Pissarra LS, Farinha CM, Liu J, Cai Z, Thibodeau PH, Amaral MD and Sheppard DN (2014) Revertant mutants modify, but do not rescue, the gating defect of the cystic fibrosis mutant G551D-CFTR. *J Physiol* **592**(Pt 9): 1931-1947.

Yeh HI, Yeh JT and Hwang TC (2015) Modulation of CFTR gating by permeant ions. *J Gen Physiol* **145**(1): 47-60.

Yu H, Burton B, Huang CJ, Worley J, Cao D, Johnson JP Jr, Urrutia A, Joubran J, Seepersaud S, Sussky K, Hoffman BJ, Van Goor F. (2012) Ivacaftor potentiation of multiple CFTR channels with gating mutations. *J Cyst Fibros* **11**(3): 237-245.

Yu Y-C, Sohma Y and Hwang T-C (2016) On the mechanism of gating defects caused by the R117H mutation in cystic fibrosis transmembrane conductance regulator. *J Physiol*: doi: 10.1113/JP271723.

Zhang ZR, Zeltwanger S and McCarty NA (2000) Direct Comparison of NPPB and DPC as Probes of CFTR Expressed in Xenopus Oocytes. *J Membr Biol* **175**(1): 35-52.

Zhou J-J, Li M-S, Qi J and Linsdell P (2010) Regulation of conductance by the number of fixed positive charges in the intracellular vestibule of the CFTR chloride channel pore. *J Gen Physiol* **135**(3): 229-245.

Zhou Z, Wang X, Liu H-Y, Zou X, Li M and Hwang T-C (2006) The two ATP binding sites of cystic fibrosis transmembrane conductance regulator (CFTR) play distinct roles in gating kinetics and energetics. *J Gen Physiol* **128**(4): 413-422.

Zielenski J and Tsui LC (1995) Cystic fibrosis: genotypic and phenotypic variations. *Annu Rev*

Genet **29**(1): 777-807.

Molecular Pharmacology Fast Forward. Published on July 13, 2016 as DOI: 10.1124/mol.116.104570
This article has not been copyedited and formatted. The final version may differ from this version.

Footnote

Wen-Ying Lin is a recipient of a scholarship (No. 102-Y-A-001) from Taipei Veterans General Hospital-National Yang-Ming University Excellent Physician Scientists Cultivation Program in Taiwan. This work is supported by [R01DK55835] from the National Institute of Health, a grant (Hwang11P0) from the Cystic Fibrosis Foundation (to T. -C. H.) and JSPS KAKENHI Grant Number [25293049], [15K15035], [16H05122] (to Y.S.). During the course of the study, 5% of the salary support for T. – C. H. was provided by Vertex Pharmaceuticals Inc.

Molecular Pharmacology Fast Forward. Published on July 13, 2016 as DOI: 10.1124/mol.116.104570
This article has not been copyedited and formatted. The final version may differ from this version.

Figure Legends

Figure 1. Dual effects of NPPB on CFTR. (A) The energetic coupling model (Jih and Hwang, 2012) for wild-type CFTR gating illustrating the relationship between opening/closing of the gate (three vertical transitions), ATP binding/unbinding (two horizontal transitions on the left), NBD dimerization/dissociation (two horizontal transitions on the right), and ATP hydrolysis and dissociation of hydrolytic products (oblique transitions in below). The yellow trapezoids represent CFTR's two TMDs, which craft a gated pore. The red and blue semicircles depict CFTR's NBD1 and NBD2 respectively. They jointly form the ATP binding site 1 (lower binding pocket), which consists of the head subdomain of NBD1 and the tail subdomain of NBD2, and catalysis-competent site 2 (upper binding pocket), composed of the head subdomain of NBD2 and the tail subdomain of NBD1. The different lengths of the arrows marking the transitions represent relatively different rate constants. The top three states represent the closed states, whereas the lower four states are open channel conformations. (B) Effects of NPPB on macroscopic WT-CFTR currents. In an inside-out patch containing multiple WT-CFTR channels, the application of 200 μM NPPB results in a net current reduction that is readily reversed upon removal of NPPB. (C) Voltage-dependent block of E1371S-CFTR by NPPB. Ramped I-V curves over ± 100 mV membrane potential show a linear I-V relationship (red) in the absence of NPPB and an outwardly rectified I-V curve (blue) in the presence of 200 μM NPPB. (D) Effects of NPPB on G551D-CFTR, a mutant with defective ATP-induced NBD dimerization. Macroscopic G551D-CFTR currents increase immediately upon applying NPPB. The inset highlights a biphasic change of the currents upon removal of NPPB, a telltale sign for a fast release of the pore block followed by a slower abolition of the potentiation effect of NPPB. Fitting the decay phase in this representative trace with a single exponential function (red line) yields a time

Molecular Pharmacology Fast Forward. Published on July 13, 2016 as DOI: 10.1124/mol.116.104570
This article has not been copyedited and formatted. The final version may differ from this version.

constant of 1.55 s (mean value of 1.67 ± 0.28, n = 6). Inh-172: a thiazolidinone CFTR inhibitor (Kopeikin et al., 2010; Ma et al., 2002). 10 μM Inh-172 is used here and throughout the other figures.

Figure 2. Effects of ATP occupancy at "site 2" of NBDs on NPPB's potentiation in G551D-CFTR. (A) A modified gating scheme for G551D-CFTR. Two NBD-dimerized states from Fig. 1A are eliminated based on our previous report (Lin et al., 2014). (B) Potentiation of G551D-CFTR currents by NPPB in the presence of 20 μM ATP. Note an increase of the G551D-CFTR currents upon changing [ATP] from 2 mM to 20 μM. By lowering [ATP], we shift the channel to states with a vacant site 2 (i.e., C_2 and O_2 in panel A). (C) Effects of NPPB in the presence of 20 μM ATP on G551D/Y1219G-CFTR, a double mutant whose ATP affinity at site 2 is drastically reduced (Zhou et al., 2006). (D) Summary of increases in P_o by NPPB under conditions marked. Fold increase in P_o: 12.1 ± 1 fold (n = 20) for G551D-CFTR in the presence of 2 mM ATP, 7.31 ± 0.81 fold (n = 3, $*p < 0.05$,) in the presence of 20 μM ATP, and 6.83 ± 1.53 fold (n = 8, $**p < 0.01$) in the presence of 20 μM ATP for G551D/Y1219G.

Figure 3. Synergistic effects of NPPB and VX-770 on G551D-CFTR. (A) A continuous recording of G551D-CFTR currents shows that the application of VX-770 further enhances G551D-CFTR current in the presence of NPPB. (B) Increase of VX-770-activated G551D-CFTR current by NPPB. (C) Synergistic effects of VX-770 and NPPB in the presence of 20 μM ATP. A continuous recording of G551D-CFTR current shows a sequential increase of the current by 20 μM ATP, VX-770 and NPPB. (D) A bar graph summarizes the mean ± S. E. of the P_o increase in the presence of 2 mM ATP (solid bars) or 20 μM ATP (open bars) respectively by NPPB or VX-

Molecular Pharmacology Fast Forward. Published on July 13, 2016 as DOI: 10.1124/mol.116.104570
This article has not been copyedited and formatted. The final version may differ from this version.

770 or both under conditions marked. At 2 mM ATP, in the presence of NPPB, VX-770 increases the P_o of G551D-CFTR by 4.76 ± 1.75 fold (n = 5), significantly smaller than the effect of VX-770 in the absence of NPPB (*$p < 0.05$). Similarly, the presence of VX-770 significantly dampens the effect of NPPB (6.27 ± 1.0 fold, n = 9, **$p < 0.01$). Thus, an overall 46.6 ± 8.5 fold (n = 18) increase in P_o is seen with VX-770 and NPPB applied together. At 20 μM ATP, the effect of VX-770 was reduced (4.79 ± 1.04 fold, n = 14; 9.32 fold at 2 mM ATP in Fig. 4F). In the presence of VX-770, NPPB yields a 5.00 ± 0.40 fold increase of G551D currents (n = 13, *$p < 0.05$ compared to Fig. 2D); whereas VX-770 enhances the P_o of NPPB-treated G551D-CFTR by only 2.53 ± 0.31 fold (n = 3). When the two reagents were applied together, we obtained 18.0 ± 5.0 fold increase of the P_o for G551D-CFTR (n = 7).

Figure 4. Different mechanisms of action for NPPB and VX-770 on K1250A- and ΔNBD2-CFTR. (A) Slow current relaxation of K1250A-CFTR upon removal of ATP. Red line represents single-exponential fit of the current decay with a time constant of 54.1 s. (B) Effects of VX-770 on current relaxation of K1250A-CFTR upon removal of ATP. Red line indicates single-exponential fit of the current decay with a time constant of 96.4 s. (C) Effects of NPPB on current relaxation of K1250A-CFTR upon removal of ATP. Note an immediate decrease of the K1250A-CFTR currents upon the application of NPPB due to pore block. The current decay upon removal of ATP can be fitted with a single-exponential function (red line) with a time constant of 22.9 s. (D) A bar graph summarizes the current relaxation time constant of K1250A-CFTR upon ATP washout in the presence of VX-770 (solid bar, 93.2 ± 12.4 s, n = 9, *** $p < 0.001$ compared to control), NPPB (open bar, 26.9 ± 3.01 s, n = 9, *** $p < 0.001$ compared to control), and control (hatched bar, 55.6 ± 4.31 s, n = 19). (E) Effects of NPPB on ΔNBD2-CFTR.

Molecular Pharmacology Fast Forward. Published on July 13, 2016 as DOI: 10.1124/mol.116.104570
This article has not been copyedited and formatted. The final version may differ from this version.

Macroscopic ΔNBD2-CFTR currents decrease immediately upon applying NPPB. The calculated gating effect of NPPB on ΔNBD2-CFTR was only 2.56 ± 0.15 fold (n = 5, *** $p < 0.001$). A biphasic change of the ΔNBD2-CFTR currents is shown upon NPPB removal due to a fast release of blockade followed by a slower abolition of the potentiation effect. The slow decay phase can be fitted by a single exponential curve with time course of 39.7 s (mean value: 39.65 ± 6.68 s, n = 9). (F) Summary of effects of VX-770 (solid bar) and NPPB (open bar) on G551D- and ΔNBD2-CFTR.

Figure 5. ATP concentrations influence the effects of NPPB on WT-CFTR gating. (A) Effects of NPPB on WT-CFTR at 100 μM ATP. A continuous recording of WT-CFTR shows a decrease of macroscopic currents by lowering [ATP] from 2 mM to 100 μM. Subsequent application of NPPB results in a net decrease of the currents, indicating blocking effects outweigh the gating effect. The calculated gating effect of NPPB was 2.37 ± 0.17 fold (n = 7). (B) Similar experiments as that in panel A except [ATP] = 20 μM ATP when NPPB was added. The calculated gating effect was 3.40 ± 0.24 fold (n = 5). (C) Effects of NPPB on WT-CFTR gating at 5 μM ATP, with a calculated gating effect of 5.19 ± 0.60 fold (n = 8). (D) Effects of NPPB on Y1219F at 100 μM ATP, with a calculated gating effect of 2.95 ± 0.43 fold (n = 5). (E) Effects of NPPB on Y1219F-CFTR at 5 μM ATP, with a calculated gating effect of 9.10 ± 1.93 fold (n = 9). (F) A bar graph summarizes the gating effects of NPPB under different ATP concentrations for WT- (solid bars) or Y1219F-CFTR (open bars). Calculated gating effects of NPPB on Y1219F-CFTR at 2 mM and 20 μM ATP were 1.92 ± 0.23 fold (n = 8) and 5.41 ± 0.98 fold (n = 6) respectively.

Molecular Pharmacology Fast Forward. Published on July 13, 2016 as DOI: 10.1124/mol.116.104570
This article has not been copyedited and formatted. The final version may differ from this version.

Figure 6. A modified gating model of CFTR. This gating scheme modified from Jih and Hwang (2012) incorporates the mechanism for ATP-dependent inhibition of G551D gating in our previous study (Lin et al., 2014) as well as data in the current report. Two states, O_0 and C_{0AD}, with NBD-dimerized but a vacant ATP binding site 2, are added to accommodate the mechanism of NPPB in G551D and to explain the biphasic current decay after ATP washout in G551D in previous study (Lin et al., 2014). These two newly added states are simple mirror images of O_1 and $C_{2\,AD}$. The idea of energetic coupling between NBD dimerization and gate opening predicts that O_1 and O_0 are two stable open states.

Figure 1

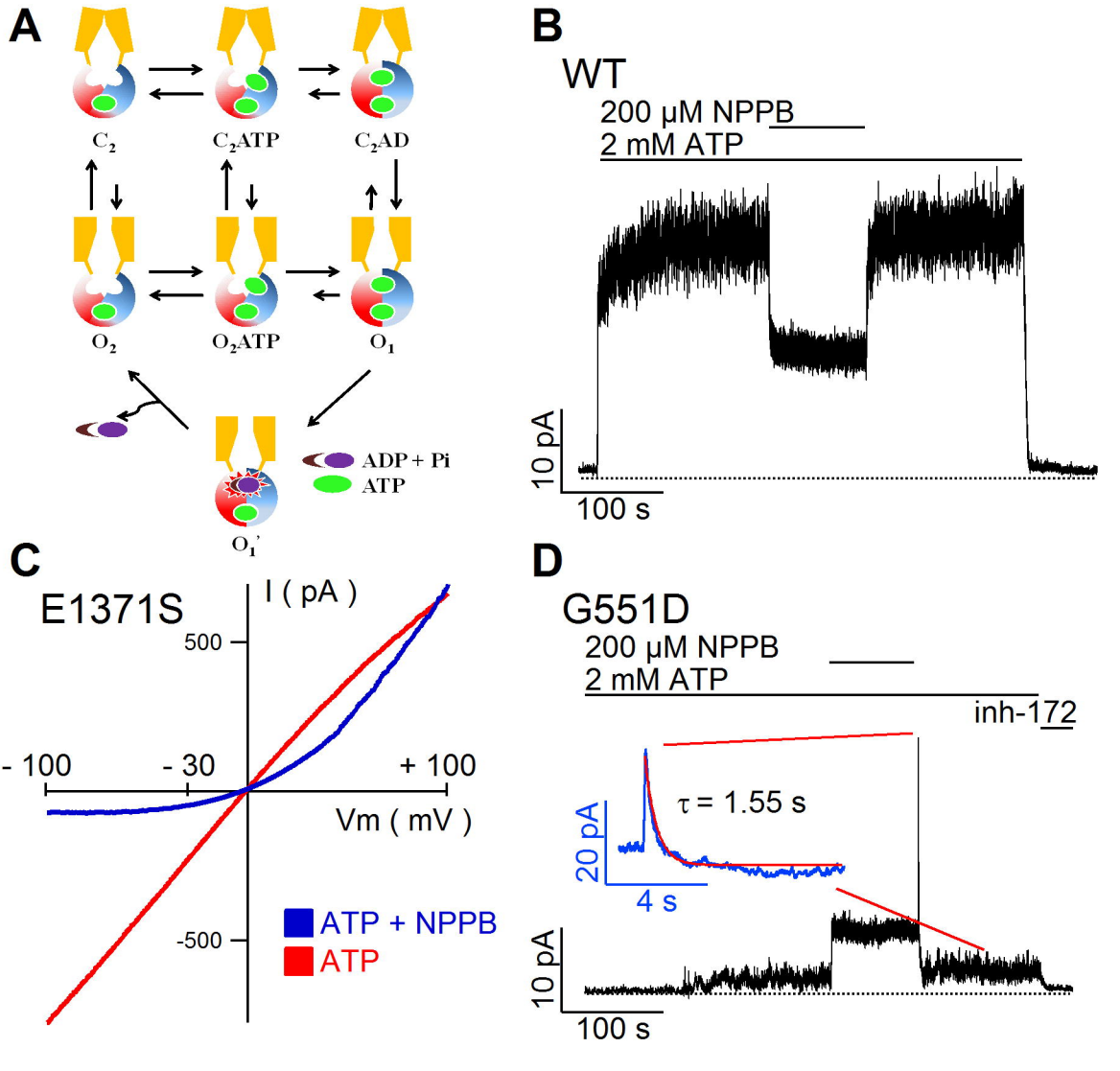
A
C2
C2ATP
C2AD
O2
O2ATP
O1
O1'
ADP + Pi
ATP
B
WT
200 µM NPPB
2 mM ATP
10 pA
100 s
C
E1371S
I (pA)
500
- 100
- 30
+ 100
Vm (mV)
-500
ATP + NPPB
ATP
D
G551D
200 µM NPPB
2 mM ATP
inh-172
τ = 1.55 s
20 pA
4 s
10 pA
100 s

Figure 2

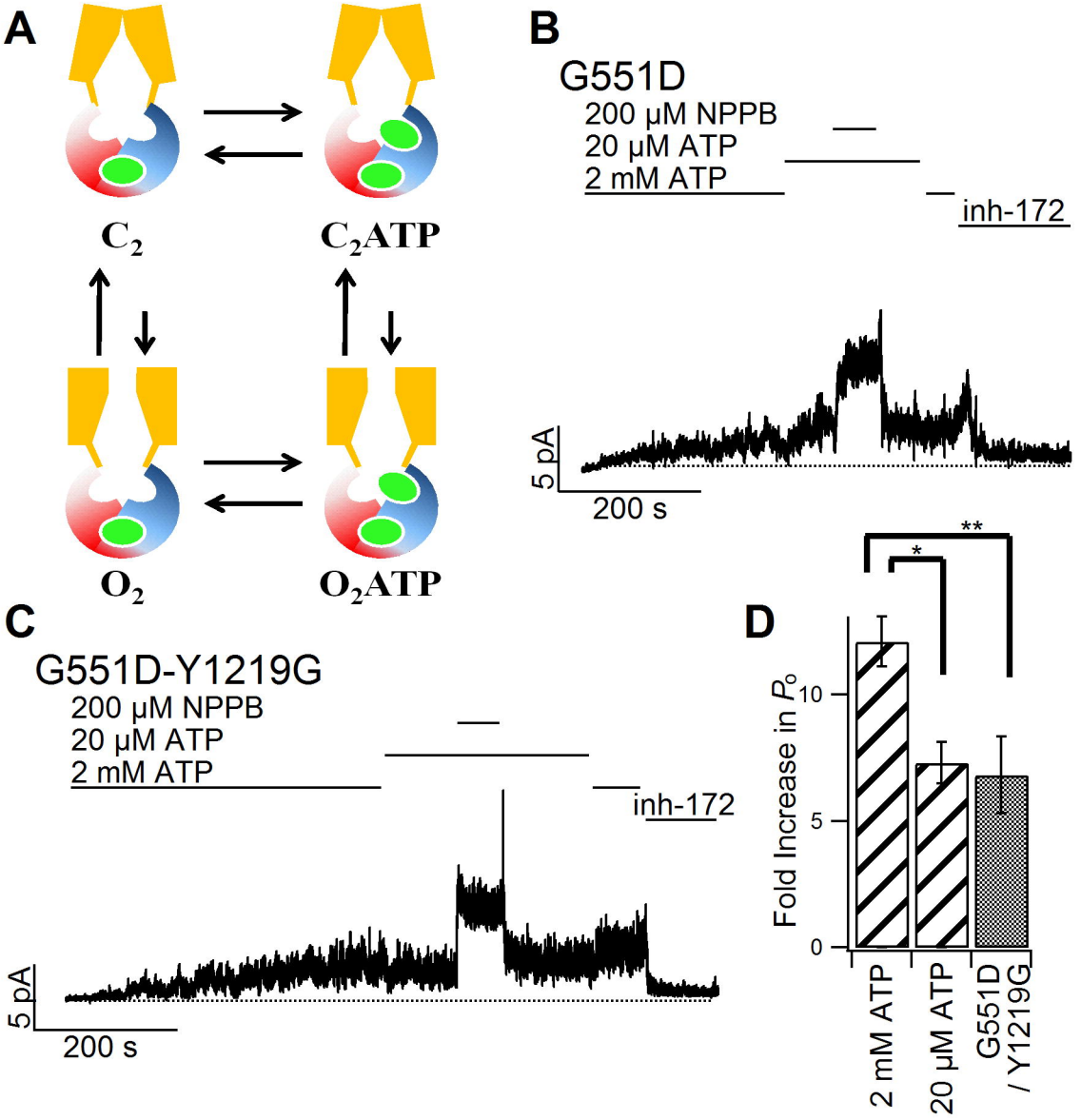
A
C2
C2ATP
O2
O2ATP
B
G551D
200 μM NPPB
20 μM ATP
2 mM ATP
inh-172
5 pA
200 s
C
G551D-Y1219G
200 μM NPPB
20 μM ATP
2 mM ATP
inh-172
5 pA
200 s
D
**
*
Fold Increase in Po
10
5
0
2 mM ATP
20 μM ATP
G551D / Y1219G

Figure 3

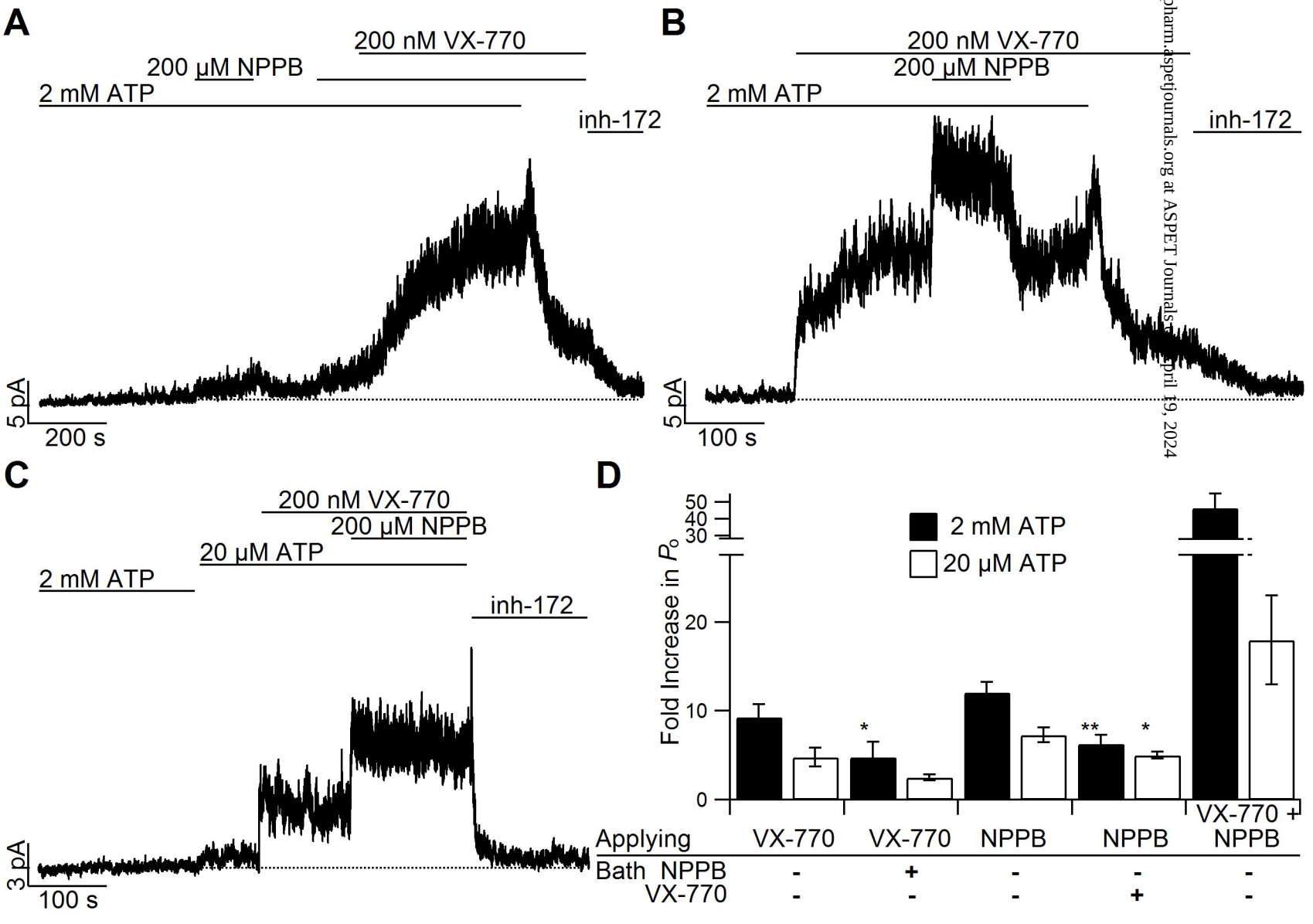

Figure 4

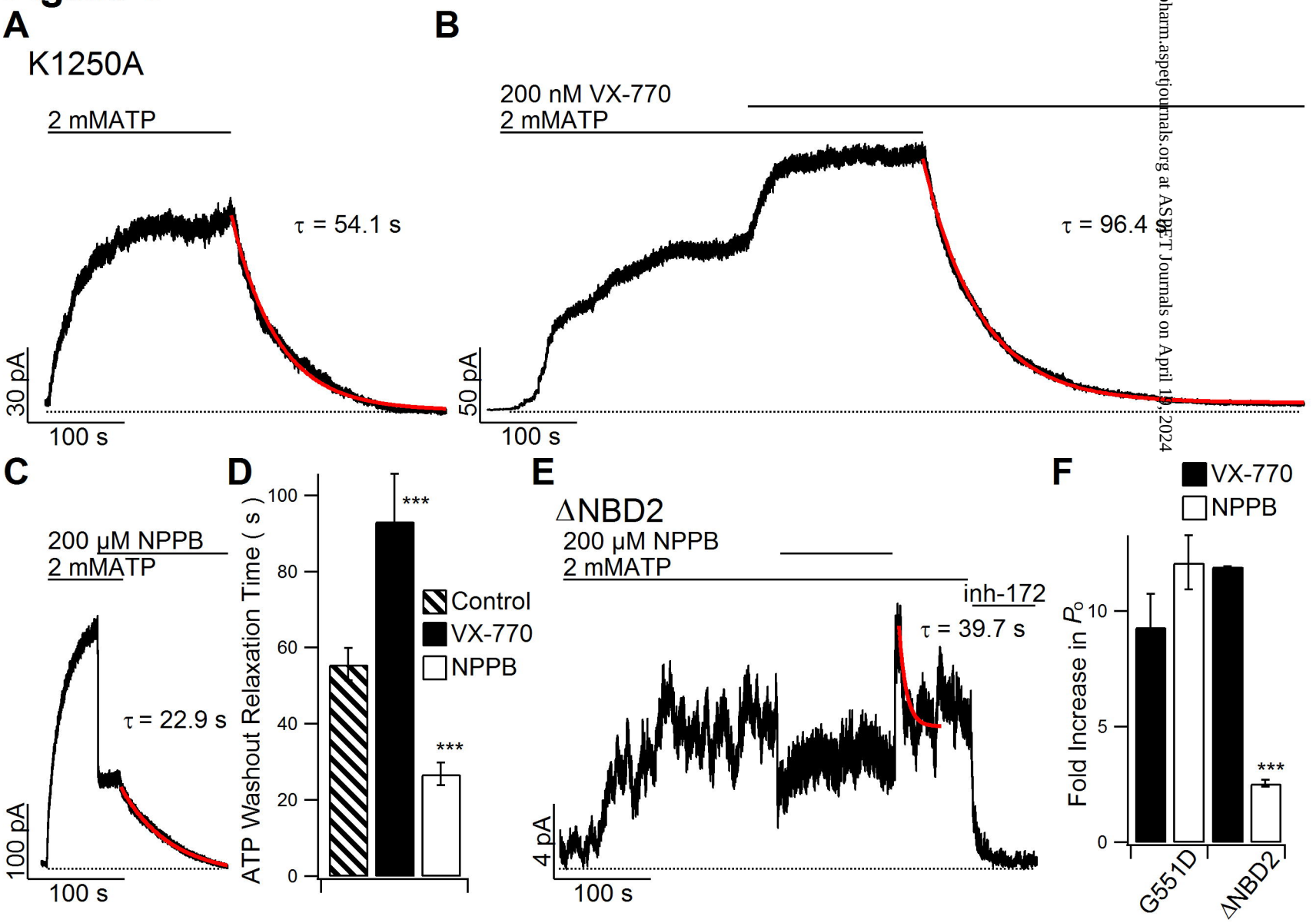

Figure 5

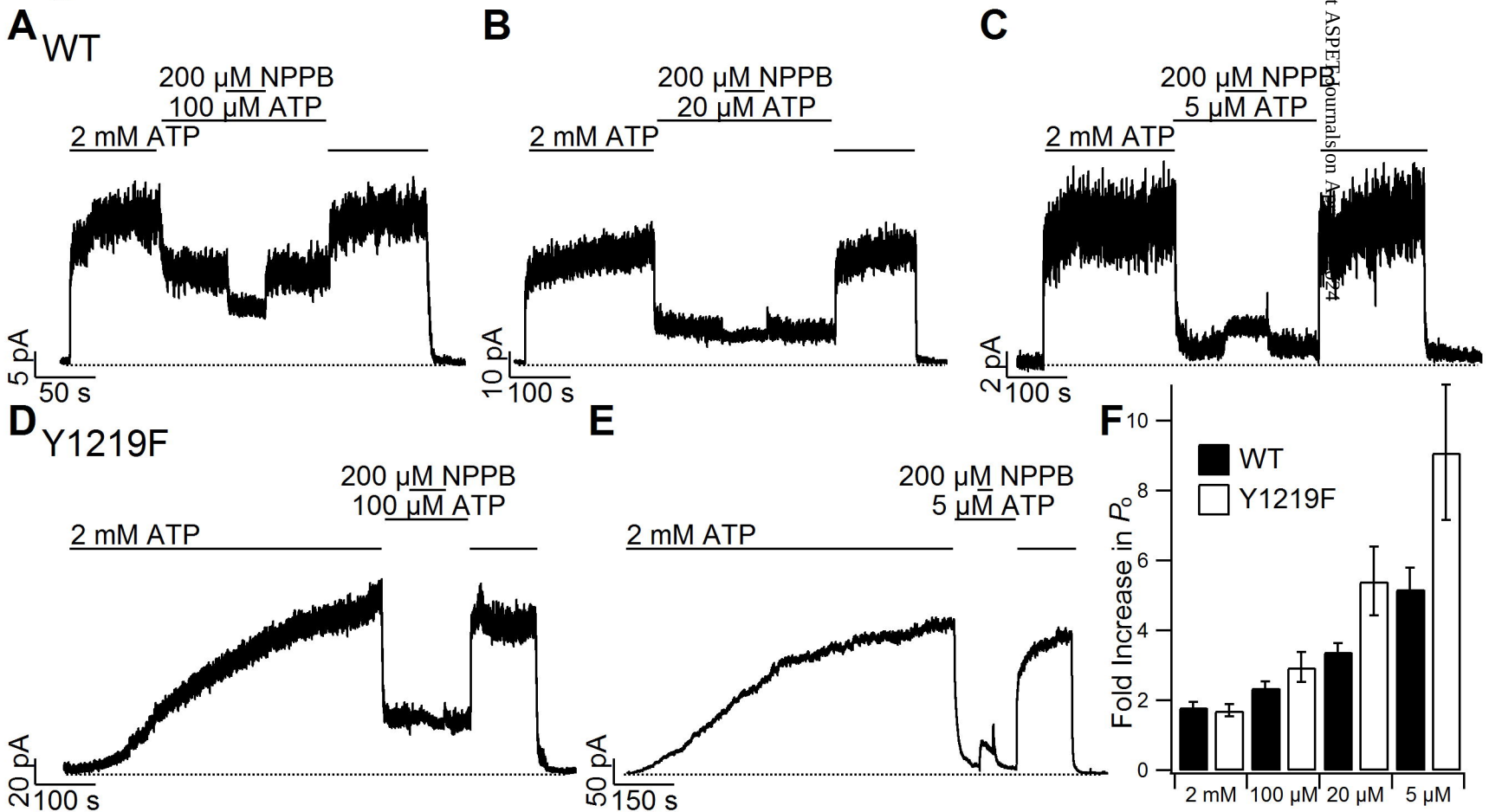

Figure 6